

Optimization of Process Variables in Copper Infiltration of Low and High Density Ferrous Structural Parts

Jessu Joys^{1,a} and Sydney Luk^{1,b}

¹United State Bronze Powders, Inc., 408 Route 202, Flemington, NJ 08822, USA
^ajessu.joys@usbronzepowders.com, ^bsydney.luk@usbronzepowders.com

Abstract

Copper infiltration is demonstrated as a viable solution to achieve higher mechanical properties by filling the interconnected porosities of a ferrous structure with copper infiltrant. This paper will present the results of a design of experiments study based on the selected processing variables in the copper infiltration process. The variables are the following: Infiltrating temperatures, infiltrating time at pre-heat zone and hot zone, the green density of iron part, the migration of copper into the iron part at different processing conditions. The results show the flexibility of the infiltration process to attain certain mechanical properties by changing the processing conditions.

Keywords : Copper Infiltration, Process Optimization, ferrous p/m, Dimensional Change Control, Rockwell Hardness

1. Introduction

Copper infiltration is demonstrated as a viable solution to achieve higher mechanical properties by filling the interconnected porosities of a ferrous structure with copper infiltrant. In this process molten copper is absorbed into the porosities of the iron matrix by capillary reaction. The resulting part will have a higher sintered density with significantly higher mechanical properties. Semlak and Rhines¹ derived a general equation to calculate rate of rise of a liquid metal flow through a wetted porous skeleton:

$$h = \frac{2}{\Pi} \left(\sqrt{\frac{Rc \times \cos \theta \times \gamma \times t}{2\eta}} \right) \quad (1)$$

h = height of rise of the liquid, t = time of rise, γ = surface tension, η = liquid viscosity, Rc = average capillary radius of a porous skeleton, θ = wetting angle

In our previous study the key processing factors were discussed in infiltration and presented case studies from industry to demonstrate “good” and “bad” infiltration². This study is focused on the key infiltration parameters such as the infiltrating (hot zone) temperature, infiltrating time, pre-sintering (pre-heat) time, and the green densities of the iron part. These variables can be adjusted in the manufacturing process to optimize the mechanical properties, dimensional change and processing cost.

2. Experimental and Results

The study is the summary of a statistically designed experiment using four different processing variables and two types of infiltrants. Operating ranges for each parameter were selected. Standard F-0008 iron mix was used to make the transverse bars (1.25”X0.5”X0.5”) in all the cases. Please see the list of selected processing variables and their ranges below (Table 1).

Table 1. Processing variables

	Operating range
Pre-sintering time, (minutes)	7 – 21
Infiltrating time, (minutes)	20 – 50
Infiltration temperature, (F)	2025 – 2075
Green density of the iron part (g/cc)	6.2 – 6.8

The experiments were designed and analyzed using Stat-Ease Design-Expert Version 5.0.10 software. The infiltration efficiency, hardness and dimensional changes of the infiltrated parts were the tested. The experiments were conducted in a tube furnace (3” diameter) at the research lab of United State Bronze Powders, Inc. The infiltrating atmosphere was dissociated ammonia (75%H₂/25%N₂) with a constant gas flow of 50scfh.

Two types of infiltrants were used in this study, a powder infiltrant (XF-3) and a paste infiltrant (XF-P) with 5-7% of liquid fraction.

Figure 1 and Figure 2 illustrates the hardness of the infiltrated part on Z axis versus the pre-sintering time and the infiltrating time on the X and Y axis respectively. The

graphs illustrates that the same hardness can be achieved by infiltrating the part at a shorter time and higher temperature (Fig. 1) compared a lower temperatue and longer time (Fig. 2). A series of 3D design diagrams were created using the Design-Expert software which shows the similar trends.

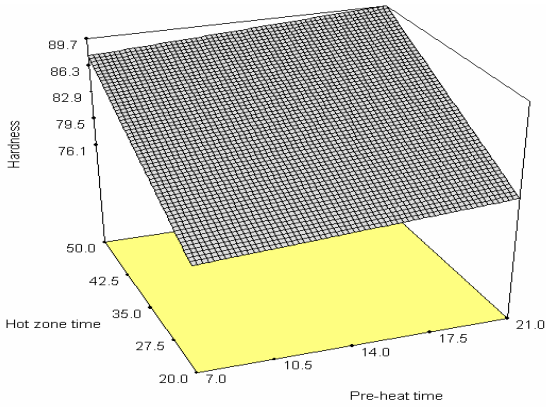


Fig. 1. Rockwell Hardness (B scale) of XF-3 infiltrated part pressed at a green Density of 6.8g/cc and infiltrated at a temperature of 2025F.

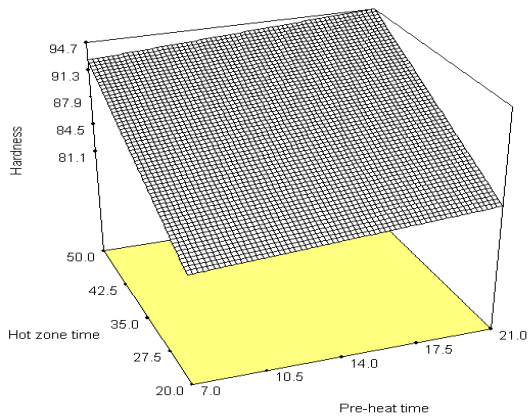


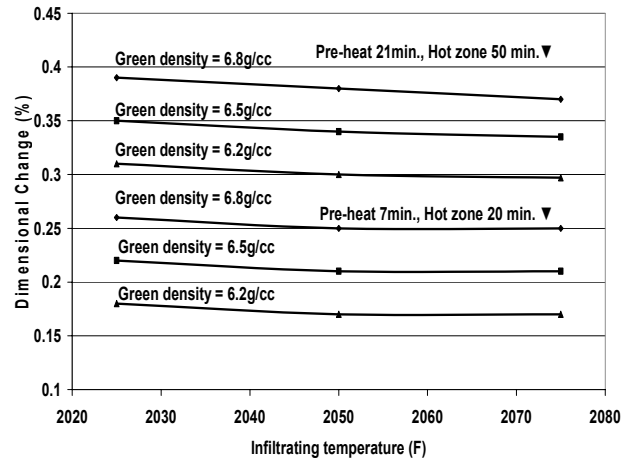
Fig. 2. Rockwell Hardness (B scale) of XF-3 infiltrated part pressed at a green Density of 6.8g/cc and infiltrated at a temperature of 2075F.

The hardness of the top and bottom of the infiltrated parts were measured as a qualitative way of looking at the filling of the open pores with molten copper. The variation in hardness between the top and bottom surface of the test bars were very minimal for the parts pressed to the highest green density (6.8g/cc) and infiltrated at a longer time at a high temperature (2075F). The hardness variation was the maximum for the parts pressed at the lower green density (6.2g/cc) and infiltrated for the shortest infiltrating time at the highest temperature (2075F).

Graph1 shows that the dimensional change can be controlled by changing the green density of the iron part, changing the infiltration time or infiltration temperature.

Figure 3 illustrates the higher hardness values can be achieved by using a shorter pre-heating time during the infiltration process.

Dimensional Change % of parts infiltrated at different processing conditions



Graph 1. Dimensional change of XF-3 infiltrated parts at different processing conditions.

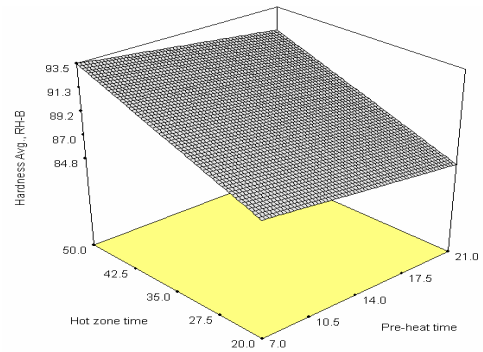


Fig. 3. Rockwell Hardness (B scale) of XF-P infiltrated part pressed at a green Density of 6.8g/cc and infiltrated at a temperature of 2050F 3.

3. Summary

The studies show higher mechanical properties can be achieved by optimizing the key processing variables. The parts pressed at a constant green density and infiltrated using XF-3 at different temperatures showed a minimum dimensional variation over the temperature range, 2025F to 2075F.

4. References

1. K.A. Semlak and F.N. Rhines, The rate of Infiltration of Metals, Trans. Inst. Min. Met. Eng., p 325 (1958).
2. J. Joys and S. Luk, Proceedings of the 2005 International conference of PM and Particulate Materials, Part 6, p 91 (2005).